Experimental Research on the Milling Process of Some Composite Materials

GHEORGHE VASILE[1], CATALIN FETECAU [2]*, DUMITRU AMARANDEI[3], ALEXANDRU SERBAN[4]

[1] Technical University of Pitesti, Department of Technologies and Management, 1 Targul din Vale Str., 110040, Pitesti, Romania

[2] Dunarea de Jos University of Galati, Department of Manufacturing, Robotics and Welding Engineering, 47 Domneasca Str., 800008, Galati, Romania

[3] Stefan cel Mare University of Suceava, Department of Engineering and Management of Technological Systems, 13 Universitatii Str., 720229, Suceava, Romania

[4] Transilvania University of Brasov, Department of Installations for Civil Engineering, 29 Eroilor Str., 500036, Brasov, Romania

Milling is a very common process in the manufacture of plastic parts. In a technological process, milling may be the final procedure, consequently influencing the quality of the product. To determine the optimum processing conditions, it is necessary to make an accurate model of the forces in order to describe the process in terms of cutting parameters. Experimental research has been conducted on the influence of the cutting parameters on the milling cutting force components. This paper aims to obtain the equations that define the variation of the cutting force components by the milling process parameters in the processing of specimens of polyamides (PA66, PA66-GF30 and MoS_2. These polyamides belong to the class of technical plastics and are thermoplastics with excellent mechanical properties, also used in the engineering industry.

Keywords: Modeling, face milling, polyamide

Since their appearance, polyamides have known a growing use in various branches of engineering, such as aerospace engineering, machine building, robotics, etc. At present, over 80% of the structure of the products manufactured and used contain plastic parts, usually obtained by injection, although sometimes milling operations are also necessary to obtain the final part [12,13, 17].

The assessment of processability can be made applying numerous criteria of which the most important are: tool life, cutting forces, power consumption, specific cutting force and machined surface roughness [4,10,11,15,16].

The milling process represents about 25% of the cutting machining for polyamides. Due to this growing use of polyamides, it is necessary to study the behavior of these materials during the cutting process [3, 5, 10]. The research conducted so far has focused on the processing by milling of materials with similar properties to those of polyamides. During these studies, the cutting forces, the chip formation as well as the roughness of the surface obtained have been investigated according to the material of the tool used, their type and geometry and the cutting parameters of the system [6,8,9].

So far, there are no studies in the literature regarding the cutting forces that occur in the milling of polyamides. Further on, the study provides information about the milling of plastic composites fiberglass reinforced in the experimental works of Davim, Reis and Antonio [7]. The two materials studied were the 65% glass-fiber reinforced polyester, the unsaturated polyester Viapal VUP 9731 and polyester ATLAC 382-05.

Experimental research has shown that the material of the processed specimen influences the three components of the cutting force occurring in the milling of Viapal VUP 9731 and ATLAC 382-05 [7]. The cutting parameters used in the experiments are: single cutting depth, t = 2 mm, longitudinal feed, f = 0.04, 0.08, 0.12 mm/rev; cutting speed, v = 47, 79, 110 m/min; cutting tool used: end mill with 30° inclination angle and 7° clearance angle. The following conclusions resulted: in the processing of polyesters, for speeds between 47 and 110 (m/min) and feeds between 0.04 and 0.12 (mm/rev), the resulting forces are between 17 and 54 N [7]; it is observed that the cutting force increases with the increase of the feed and decreases with the cutting speed [7]; also, the cutting force in the processing of ATLAC 382-05 is smaller than that of Viapal VUP 9731, under the same cutting conditions due to the more pronounced elastic behaviour of polyamide Viapal VUP 9731 [7].

Fetecau and Stan [2] conducted research on the turning of PTFE composites using polycrystalline diamond tools in order to analyze the effect of the cutting parameters and the edge radius of the cutting plate on the forces resulted and the roughness of the surface processed.

The main purpose of this paper is to obtain the equations that define the variation of the cutting force components by the milling process parameters in the processing of specimens of polyamides PA66, PA66-PA66 GF30 and MoS_2.

Experimental part

Cutting process modeling through composite polyamide milling

For the experimental research on polyamide cutting, the empirical model was adopted (fig. 1).

The input values varied were: material of the processed part; cutting speed, *v*, [m/min]; longitudinal feed, *f*, [mm/rev]; cutting depth, *t*, [mm].

Three widely used polyamides (PA66, PA66-GF30 and MoS_2) were considered. The first is the base and the other two are improvement elements.

The output result was:

- the milling cutting force defined by its three components, F_x, F_y and F_z.

* email: Catalin.Fetecau@ugal.ro

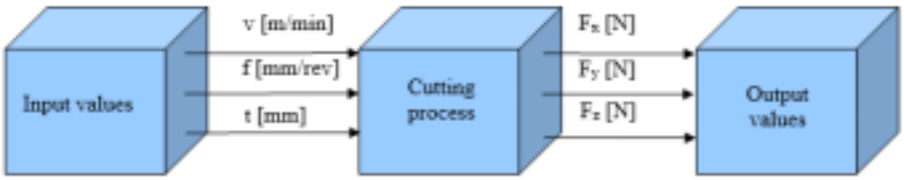

Fig. 1. Schematic empirical model of the cutting process

The linear model was adopted to describe the dependence of output on input parameters for each material investigated, a model widely used in modeling the cutting process. Considering that the input variables are independent, the equations of the milling cutting force components are of the form

$$F_z = C_z + a_z \cdot t + b_z \cdot f + c_z \cdot v + d_z \cdot t \cdot f + e_z \cdot t \cdot v + g_z \cdot f \cdot v \quad [N],$$
$$F_y = C_y + a_y \cdot t + b_y \cdot f + c_y \cdot v + d_y \cdot t \cdot f + e_y \cdot t \cdot v + g_y \cdot f \cdot v \quad [N],$$
$$F_x = C_y + a_y \cdot t + b_y \cdot f + c_y \cdot v + d_z \cdot t \cdot f + e_z \cdot t \cdot v + g_z \cdot f \cdot v \quad [N], \quad (1)$$

where:

C, a, b, c, d, e, g are constants to be determined based on experimental data;

t - cutting depth, in [mm];

f - feed per rotation of the workpiece, in [mm/rev];

v - cutting speed, in [m/min].

The other parameters related to the cutting tool and the cooling conditions were held constant.

Experiment plan used in the experimental research

The comprehensive factorial plan type 3^3 has been adopted, with repeated experiments in each point, presented by Vasile, Fetecau and Serban [1].

Methodology used for experimental data processing

The force depends on several variables of the cutting process: feed, cutting depth, cutting speed. In the study, the influence of the cutting parameters characterizing the cutting process on the force is analyzed considering the interaction between the parameters mentioned. A separate study of the influences affecting the characterization accuracy of the measured force. If the force is denoted by *Y*, and the other variables by X_1, X_2, X_3, etc., a function $Y = f(X_1, X_2, X_3, ...)$ is obtained.

In the case of the dependence between three input variables, the *Y* output size is given by the equation

$$Y = A_0 + A_1X_1 + A_2X_2 + A_3X_3 + A_{12}X_1X_2 + A_{13}X_1X_3 + A_{23}X_2X_3 + A_{123}X_1X_2X_3. \quad (2)$$

Having in this case eight coefficients to determine, the system of equations resulting from the application of the method of least squares will have 8 equations. The number of experiments should be higher so as to estimate the coefficients.

Data processing will be carried out using the ANOVA method, also known as dispersional analysis or analysis of variance [1].

Methods and means used in the experimental research

Specimens

Regarding the dimensions of the specimen, the width *l* is established by the tool diametre, $l=(0.6 \div 0.8)D$ (SR ISO 8688-1). For the tool diametre $D=121$ mm, $l=78$mm results. 85 mm will be adopted.

The specimens used in the experiments are like those shown in figure 2.

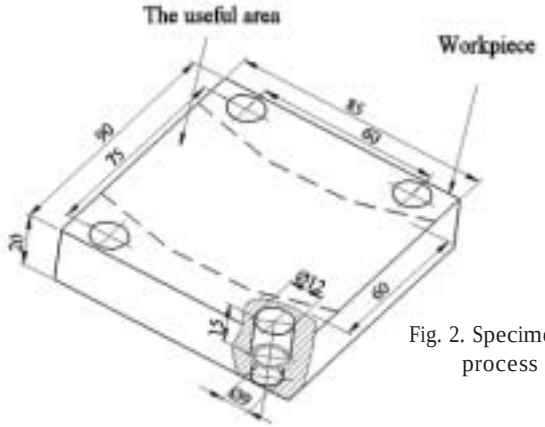

Fig. 2. Specimen to process

The processing scheme and the material of the specimens used were presented by Vasile, FetecAu and Serban [1].

Cutting tool

A mill consisting in body 2 and a single detachable plate 1 were used (fig. 3).

Cutting plates

Considering the recommendations of certain companies and the supply possibilities, a SEMN 12 04 AZ plate, produced by SANDVIK Coromant, was used. The shape of the body and the dimensions of the plate are shown in figure 5.

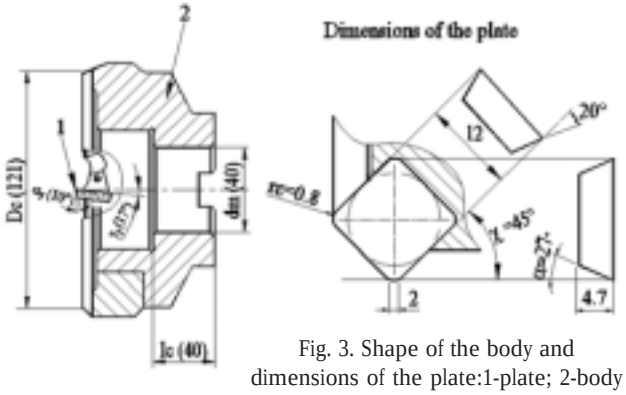

Fig. 3. Shape of the body and dimensions of the plate:1-plate; 2-body

The functional geommetry of the plate was presented by Vasile, Fetecău and ªerban [1].

Equipment used to measure the cutting force components

To determine the cutting force components, a Kistler 92578 piezoelectric dynamometer was used, which offers the possibility to record forces and momentes on the three cutting directions. Data acquisition was performed with a computer and a Kistler DynoWare data acquisition program. The figure below shows the system for measuring the forces and the directions of the cutting force components by the Kistler dynamometer.

Specimen orientation and fixing on the Kistler dynamometer is made with 4 M8 screws, as in scheme in figure 5. The cutting forces will be recorded in the useful area of the specimen, to avoid errors due to the screw bores.

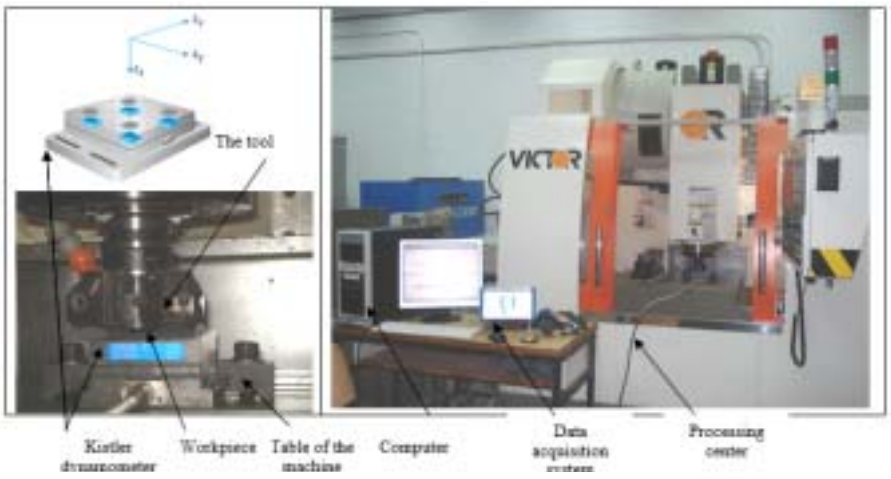

Fig. 4. System for force measurement

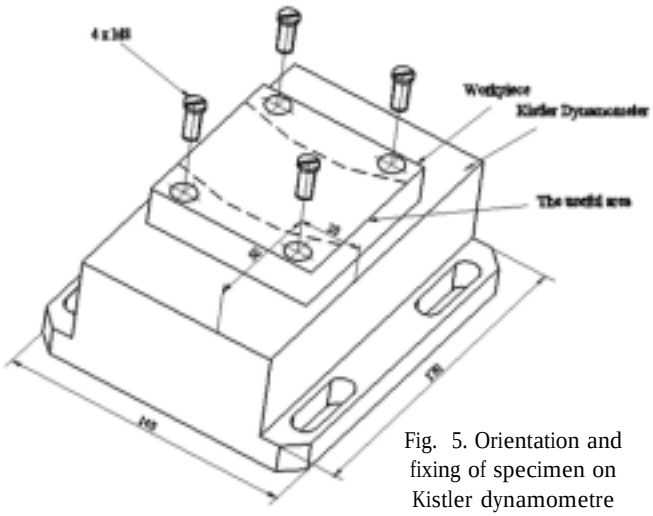

Fig. 5. Orientation and fixing of specimen on Kistler dynamometre

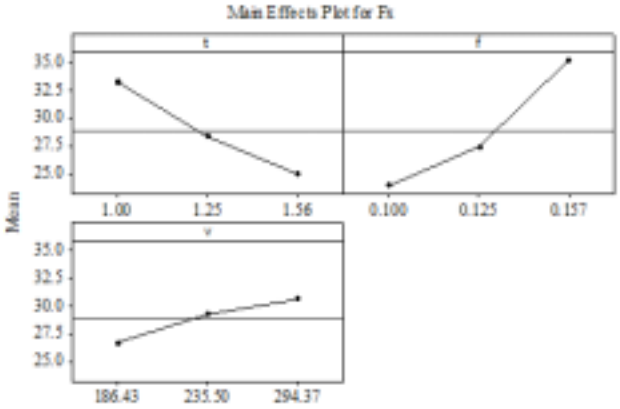

Fig. 6. Graph of the effects of the three parameters for the cutting force F_x when milling PA 66

Independent variables / Level	v, [m/min]	f_n, [mm/th]	t, [mm]
Superior (+1)	294.37	0.157	1.56
Medium (0)	235.5	0.125	1.25
Inferior (-1)	186.43	0.1	1

Table 1
VALUES OF PROCESSING PARAMETERS

Exp. no.	Levels t	f	v	F_x N	S/N ratio dB	F_y N	S/N ratio dB	F_z N	S/N ratio dB
1	-1	1	1	**50.28**	-34.0279	**117.14**	-41.3741	**90.93**	-39.1741
2	-1	1	0	**42.52**	-32.5719	**102.50**	-40.2145	**83.13**	-38.3952
3	-1	1	-1	**33.07**	-30.3887	**84.20**	-38.5062	**66.35**	-36.4368
4	-1	-1	1	**28.31**	-29.0388	**71.53**	-37.0898	**79.68**	-38.0270
5	-1	-1	0	**27.62**	-28.8245	**70.93**	-37.0166	**77.03**	-37.7332
6	-1	-1	-1	**25.31**	-28.0658	**68.17**	-36.6719	**74.1**	-37.3846
7	-1	0	1	**33.84**	-30.5886	**92.55**	-39.3275	**81.43**	-38.2157
8	-1	0	0	**30.84**	-29.7823	**81.30**	-38.2018	**76.43**	-37.6653
9	-1	0	-1	**29.68**	-29.4493	**71.30**	-37.0618	**60.47**	-35.6308
10	0	1	1	**33.17**	-30.4149	**125.84**	-41.9964	**92.66**	-39.3378
11	0	1	0	**32.52**	-30.2430	**124.67**	-41.9152	**78.49**	-37.8963
12	0	1	-1	**31.68**	-30.0157	**121.45**	-41.6880	**77.14**	-37.7456
13	0	-1	1	**24.23**	-27.6871	**129.76**	-42.2628	**83.69**	-38.4535
14	0	-1	0	**23**	-27.2346	**123.54**	-41.8362	**80.56**	-38.1224
15	0	-1	-1	**22.4**	-27.0050	**117.76**	-41.4200	**77.37**	-37.7715
16	0	0	1	**25.9**	-28.2660	**124.84**	-41.9271	**86.11**	-38.7011
17	0	0	0	**24.46**	-27.7691	**122.95**	-41.7946	**79.62**	-38.0204
18	0	0	-1	**23.69**	-27.4913	**118.26**	-41.4568	**76.38**	-37.6596
19	1	1	1	**34.78**	-30.3122	**158.02**	-43.6950	**104.22**	-40.3590
20	1	1	0	**31.07**	-29.8468	**152.85**	-43.6853	**93.49**	-39.4153
21	1	1	-1	**30.54**	-29.6974	**149.55**	-43.4957	**91.37**	-39.2161
22	1	-1	1	**23.58**	-27.4509	**168.99**	-44.5572	**98.39**	-39.8590
23	1	-1	0	**22.12**	-26.8957	**153.32**	-43.9907	**96.42**	-39.6833
24	1	-1	-1	**21.77**	-26.7572	**154.61**	-43.7848	**91.74**	-39.2512
25	1	0	1	**21.34**	-26.5839	**155.60**	-43.8402	**89.89**	-39.0742
26	1	0	0	**23.07**	-27.2610	**130.52**	-42.3135	**85.78**	-38.6677
27	1	0	-1	**19.64**	-25.8628	**120.08**	-41.5894	**85.35**	-38.6241

Table 2
L_{27} COMPLETE FACTORIAL PLAN OF THE CUTTING FORCES AND THE S/N RATIO FOR PA 66

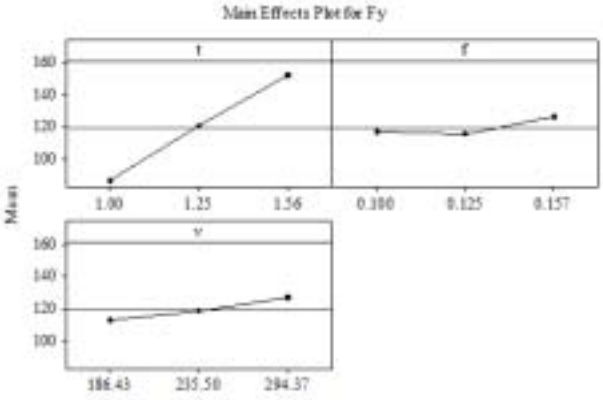

Fig. 7. Graph of the effects of the three parameters on the cutting force F_y when milling PA 66

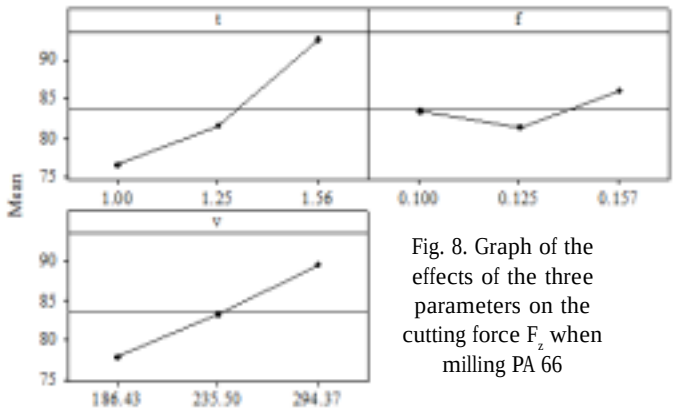

Fig. 8. Graph of the effects of the three parameters on the cutting force F_z when milling PA 66

of component F_z. The ANOVA analysis revealed that the order of influence of the three parameters on the cutting force component F_z is: cutting depth, speed, feed.

The same analysis shows the importance of each input parameter on the cutting force components in table 3. A parameter has significant effect on the cutting force component, if the value of P is less than 5%. The table represents the percentage contribution of each factor, indicating its influence on each term of the model.

The equations for the cutting milling force components are of the form:

$$F_x = -7.445 + 25.638\,t + 118.77\,f + 0.038\cdot v \ [N]. \quad (3)$$

Component	F_x		F_y		F_z	
Parameters	P-value [%]	Contribution [%]	P-value [%]	Contribution [%]	P-value [%]	Contribution [%]
t	0	27.78	0	86.17	0	55.46
f	0	54.69	0.2	2.47	0	4.64
v	0.6	6.67	0	4.08	0	29.5
t·f	15.2	2.93	0	6.13	7.6	0.99
t·v	18	2.65	45.3	0.34	0.5	2.7
f·v	17.6	2.69	75.9	0.15	0	6.09

Table 3
ANOVA ANALYSIS OF F_x, F_y,F_z for PA 66

Experimental research on surface roughness at polyamide milling

Experiment plan

The experiment plan was adopted, as described in 2.2. above. Process parameter values in their natural values correspond to the three levels (+1, 0, -1) are presented in table 1.

Results for milling forces at polyamides PA66, PA66-PA66 GF30 and MoS_2

Data processing will be performed using the ANOVA method, developed to calculate the effects of all factors and their interactions, as well as to determine the influence of the cutting parameters and their interactions, in percentages, with degrees of freedom and residues [7,12]. The analysis was performed in the Minitab 16 software.

Results and discussions

ANOVA analysis for PA 66

Table 2 summarizes the results regarding the numerical values, the mean, and the experimental values of the three components of the cutting force and the signal/noise ratio for each level of the three factors analyzed. The mean was determined by recording three values of the forces for each experiment.

To study the main effects of the process and the constructive parameters of the cutting tool on the three components of the cutting force, F_x, F_y and F_z, the graphs in figures 6-8 were constructed.

Figure 6 shows that increasing the cutting depth causes a decrease in the size of component F_x, whereas increasing the feed and the cutting speed causes an increase in the size of component F_x. The ANOVA analysis revealed that the order of influence of the three parameters on the cutting force component F_x is as follows: feed, cutting depth, cutting speed.

Figure 7 shows that increasing the cutting depth, the feed and the cutting speed causes an increase in the size of component Fy. The ANOVA analysis revealed that the order of influence of the three parameters on the cutting force component F_y is: cutting depth, speed, feed.

Figure 8 shows that increasing the cutting depth, the feed and the cutting speed causes an increase in the size

For the F_x component model, the correlation coefficient R^2 is 93.14%. The Durbin-Watson statistic index is 1.39.

$$Fy = -309.491 + 289.712\cdot t + 1775.78\cdot s + 0.271\cdot v - 1213.24\cdot t\cdot s \ [N]. \quad (4)$$

For the F_y component model, the correlation coefficient R^2 is 96.42%. The Durbin-Watson statistic index is 0.64.

$$Fz = 41.564 + 57.982\cdot t - 422.424\cdot s - 0.019\cdot v - 0.109\cdot t\cdot v + 2.107\cdot s\cdot v \ [N]. \quad (5)$$

For the F_z component model, the correlation coefficient R^2 is 92.78%. The Durbin-Watson statistic index is 1.09.

In order to make a comparison between the size of the main component F_y and the other two components, F_x and F_z, mathematical calculations were made which resulted in the following relations:

$$F_z = (0.13 - 0.42)F_y \ [N], \quad (6)$$

$$F_x = (0.57 - 0.87)F_y \ [N], \quad (7)$$

To gain an insight into the differences between the size of the forces calculated experimentally and the ones obtained through modeling, the relative error was calculated:

$$\varepsilon = \frac{Val_{exp} - Val_{model}}{Val_{exp}} * 100 \ [\%], \quad (8)$$

where:

ε is the error;

Val_{exp} – value obtained experimentally;

Val_{model} – value predicted through the linear regression model.

In the case of PA 66, the maximal relative errors calculated were: 8.86% for F_x, 7.61% for F_y and 4.73% for F_z.

ANOVA analysis for PA 66-GF 30

Table 4 presents the results regarding the numerical values, the mean and the experimental values of the three components of the cutting force, and the S/N ratio for each level of the three factors analysed. The mean was

Exp. no.	Levels t	f	v	F_x N	S/N ratio dB	F_y N	S/N ratio dB	F_z N	S/N ratio dB
1	-1	1	1	**77.7**	-37.8084	**192.11**	-45.6710	**125.40**	-41.9660
2	-1	1	0	**70.9**	-37.0129	**150.70**	-43.5623	**87.50**	-38.8402
3	-1	1	-1	**64.4**	-36.1777	**113.06**	-41.0662	**56.40**	-35.0256
4	-1	-1	1	**69.1**	-36.7896	**171.80**	-44.7005	**77.96**	-37.8374
5	-1	-1	0	**65.6**	-36.3381	**108.04**	-40.6717	**56.60**	-35.0563
6	-1	-1	-1	**63.14**	-36.0061	**49.20**	-33.8393	**37.12**	-31.3922
7	-1	0	1	**61.75**	-35.8127	**151.38**	-43.6014	**100.73**	-40.0632
8	-1	0	0	**58.26**	-35.3074	**97.03**	-39.7381	**67.83**	-36.6284
9	-1	0	-1	**56.81**	-35.0885	**57.03**	-35.1221	**47.83**	-33.5940
10	0	1	1	**52.57**	-34.4148	**169.68**	-44.5926	**126.68**	-42.0542
11	0	1	0	**49.92**	-33.9655	**140.16**	-42.9325	**94.98**	-39.5526
12	0	1	-1	**37.6**	-31.5038	**110.80**	-40.8908	**63.40**	-36.0418
13	0	-1	1	**46.63**	-33.3733	**172.66**	-44.7438	**76.15**	-37.6334
14	0	-1	0	**39.43**	-31.2292	**92.30**	-39.3040	**54.50**	-34.7279
15	0	-1	-1	**35.1**	-30.9061	**90.88**	-39.1694	**40.37**	-32.1212
16	0	0	1	**45.15**	-30.9185	**170.74**	-44.6467	**96.84**	-39.7211
17	0	0	0	**38.64**	-31.7407	**121.69**	-41.7051	**69.11**	-36.7908
18	0	0	-1	**36.12**	-31.1550	**92.05**	-39.2805	**54.13**	-34.6688
19	1	1	1	**38.45**	-31.6979	**250.00**	-47.9588	**156.68**	-43.9003
20	1	1	0	**28.84**	-30.0595	**183.10**	-45.2538	**111.64**	-40.9564
21	1	1	-1	**21.25**	-26.5472	**170.00**	-44.6090	**76.62**	-37.6868
22	1	-1	1	**29.49**	-31.2435	**188.32**	-45.4979	**72.19**	-37.1695
23	1	-1	0	**24.87**	-28.5854	**152.50**	-43.6654	**48.11**	-33.6447
24	1	-1	-1	**20.14**	-26.0812	**108.30**	-40.6926	**34.74**	-30.8166
25	1	0	1	**28.58**	-27.4509	**176.83**	-44.9511	**111.64**	-40.9564
26	1	0	0	**20.45**	-26.2139	**173.84**	-44.8030	**75.84**	-37.5980
27	1	0	-1	**19.83**	-25.9465	**110.88**	-40.8971	**48.67**	-33.7452

Table 4
L_{27} FULL FACTORIAL PLAN OF THE CUTTING FORCES AND OF THE S/N RATIO FOR PA 66 GF 30

determined by the recording of three values of the forces for each experiment.

To study the main effects of the process and constructive parameters on the three components of the cutting force, F_x, F_y ºi F_z, the graphs in figures 9 - 11 were constructed.

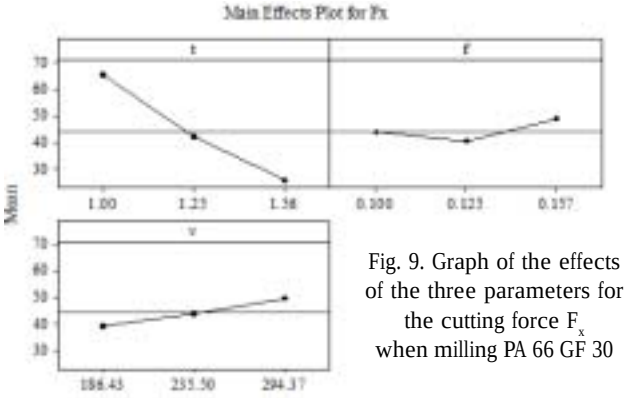

Fig. 9. Graph of the effects of the three parameters for the cutting force F_x when milling PA 66 GF 30

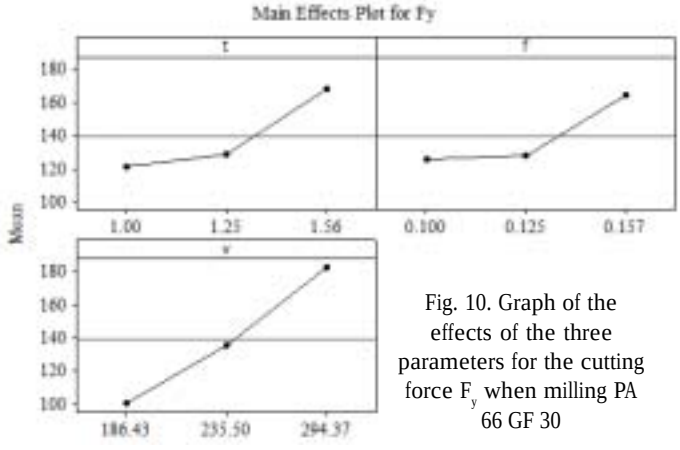

Fig. 10. Graph of the effects of the three parameters for the cutting force F_y when milling PA 66 GF 30

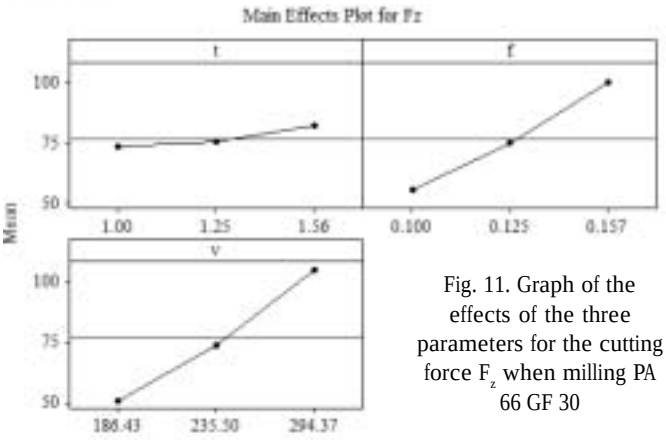

Fig. 11. Graph of the effects of the three parameters for the cutting force F_z when milling PA 66 GF 30

Figure 9 shows that increasing the cutting depth causes a decrease in the size of component F_x, whereas increasing the feed and the speed causes an increase in the component F_x. The ANOVA analysis revealed that the order of influence of the three parameters on the cutting force component F_x is: cutting depth, feed, speed.

Figure 10 shows that increasing the cutting depth, the feed and the speed causes an increase in the size of component F_y. The ANOVA analysis revealed that the order of influence of the three parameters on the cutting force component F_y is: speed, cutting depth, feed.

Figure 11 shows that increasing the cutting depth, the feed and the speed causes an increase in the size of component F_z. The ANOVA analysis revealed that the order of influence of the three parameters on the cutting force component F_z is: speed, feed, cutting depth.

The same analysis shows the importance of each input parameter on the cutting force components in table 5. A parameter has significant effect on the cutting force component, if the value of P is less than 5%. The table represents the percentage contribution of each factor, indicating its influence on each term of the model.

The equations of the cutting milling force components are of the form:

$$F_x = 142.202 - 80.631 \cdot t - 111.646 f - 0.1103 \cdot v + 1.040 \cdot fv \ [N]. \quad (9)$$

Component Parameters	F_x P-value [%]	F_x Contribution [%]	F_y P-value [%]	F_y Contribution [%]	F_z P-value [%]	F_z Contribution [%]
t	0	85.79	0	21.66	0.1	1.54
f	0	6.1	0	13.53	0	36.95
v	0	5.23	0	59.67	0	53.99
t·f	36.6	0.32	24.8	0.6	0	3.36
t·v	46.6	0.26	1.6	2.1	5.9	0.52
f·v	1	1.78	2.8	1.72	0	3.35

Table 5
ANOVA ANALYSIS OF F_x, F_y,F_z FOR PA 66 GF 30

For this model, the correlation coefficient R^2 is 94.5%. The Durbin-Watson statistic index is 0.8.

$$F_y = -409.391 + 134.118 \cdot t + 1130.08 \cdot s + + 1.690 \cdot v - 0.374 \cdot t \cdot v - 3.536 \cdot s \cdot v \ [N]. \quad (10)$$

For this model, the correlation coefficient R^2 is 96.73%. The Durbin-Watson statistic index is 1.65.

$$F_z = 191.212 - 135.941 \cdot t - 1733.09 \cdot s - 0.314 \cdot v + + 985.473 \cdot t \cdot s + 5.296 \cdot s \cdot v \ [N]. \quad (11)$$

For this model, the correlation coefficient R^2, used to established the quality of the model, is 98.84%. The Durbin-Watson statistic index is 1.79.

In order to make a comparison between the size of the main component F_y and the other two components, F_x and F_z, mathematical calculations were made which resulted in the following relations:

$$F_x = (0.11 - 0.6) F_y \ [N]. \quad (12)$$

$$F_z = (0.31 - 0.83) F_y \ [N]. \quad (13)$$

To gain an insight into the differences between the size of the forces calculated experimentally and the ones obtained through modeling, we calculated the relative error using relation (8). In the case of PA 66-GF 30, the maximal relative errors calculated were: 7.60% for F_x, 8.72% for F_y and 7.66% for F_z.

ANOVA analysis for PA 66 MoS

Table 6 presents the results regarding the numerical values, the mean and the experimental values of the three components of the cutting force, and the S/N ratio for each level of the three factors analysed. The mean was determined by the recording of three values of the forces for each experiment.

To study the main effects of the process and constructive parameters on the three components of the cutting force, F_x, F_y ºi F_z, the graphs in figures 12-14 were constructed.

Figure 12 shows that increasing the cutting depth, the feed and the speed causes an increase in the size of component F_x. The ANOVA analysis revealed that the order of influence of the three parameters on the cutting force component F_x is: cutting depth, feed, speed.

Figure 13 shows that increasing the cutting depth, the feed and the speed causes an increase in the size of component F_y. The ANOVA analysis revealed that the order of influence of the three parameters on the cutting force component F_y is: cutting depth, feed, speed.

Figure 13 shows that increasing the cutting depth, the feed and the speed causes an increase in the size of component F_z. The ANOVA analysis revealed that the order of influence of the three parameters on the cutting force component F_z is: cutting depth, speed, feed.

The same analysis shows the importance of each input parameter on the cutting force components in table 7. A parameter has significant effect on the cutting force component, if the value of P is less than 5%. The table represents the percentage contribution of each factor, indicating its influence on each term of the model.

Exp. no.	Levels t	f	v	F_x N	S/N ratio dB	F_y N	S/N ratio dB	F_z N	S/N ratio dB
1	-1	1	1	36.41	-31.2244	111.50	-40.9455	75.73	-37.5854
2	-1	1	0	30.75	-29.7569	107.17	-40.6015	71.04	-37.0301
3	-1	1	-1	29.37	-29.3581	102.22	-40.1907	62.83	-35.9633
4	-1	-1	1	26.34	-28.4123	104.90	-40.4155	73.31	-37.3033
5	-1	-1	0	19.01	-25.5796	94.04	-39.4663	67.66	-36.6066
6	-1	-1	-1	14.22	-23.0580	92.24	-39.2984	64.55	-36.1979
7	-1	0	1	30.47	-29.6774	109.78	-40.8105	73.78	-37.3588
8	-1	0	0	24.64	-27.8328	104.53	-40.3848	68.58	-36.7239
9	-1	0	-1	20.01	-26.0249	100.62	-40.0537	65.04	-36.2636
10	0	1	1	52.61	-34.4214	148.65	-43.4433	96.96	-39.7319
11	0	1	0	45.01	-33.0662	137.97	-42.7957	81.56	-38.2295
12	0	1	-1	43.44	-32.7578	127.76	-42.1279	78.95	-37.9470
13	0	-1	1	35.63	-31.0363	114.03	-41.1404	89.91	-39.0762
14	0	-1	0	33.76	-30.5680	105.45	-40.4609	88.97	-38.9849
15	0	-1	-1	28.12	-28.9803	97.44	-39.7747	87.56	-38.8461
16	0	0	1	38.03	-31.6025	122.41	-41.7563	86.82	-38.7724
17	0	0	0	36.87	-31.3335	125.28	-41.9576	81.83	-38.2583
18	0	0	-1	35.16	-30.9210	110.98	-40.9049	76.52	-37.6755
19	1	1	1	60.40	-35.6207	161.62	-44.1699	136.19	-42.6829
20	1	1	0	59.17	-35.4420	144.53	-43.1992	107.44	-40.6233
21	1	1	-1	57.24	-35.1540	131.31	-42.3660	92.43	-39.3163
22	1	-1	1	45.93	-33.2419	141.14	-42.9930	97.08	-39.7426
23	1	-1	0	43.46	-32.7618	126.26	-42.0253	93.88	-39.4515
24	1	-1	-1	44.59	-32.9847	116.37	-41.3168	83.68	-38.4524
25	1	0	1	55.96	-34.9576	150.77	-43.5663	108.76	-40.7294
26	1	0	0	48.41	-33.6987	134.53	-42.5764	104.48	-40.3807
27	1	0	-1	51.87	-34.2983	131.32	-42.3666	102.63	-40.2255

Table 6
L_{27} FULL FACTORIAL PLAN OF THE CUTTING FORCES AND OF THE S/N RATIO FOR PA 66 MoS_2

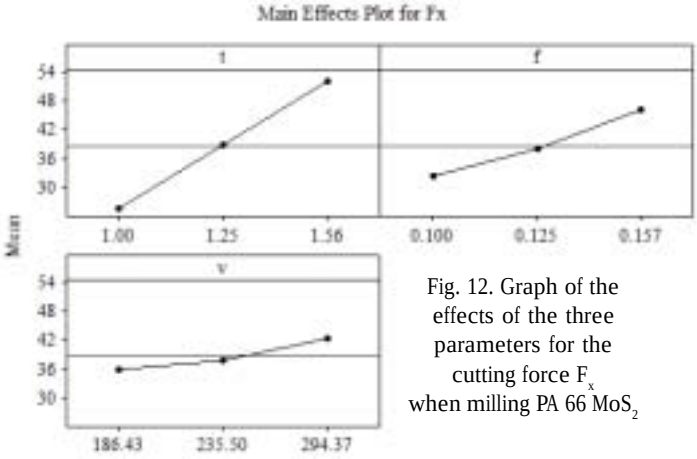

Fig. 12. Graph of the effects of the three parameters for the cutting force F_x when milling PA 66 MoS_2

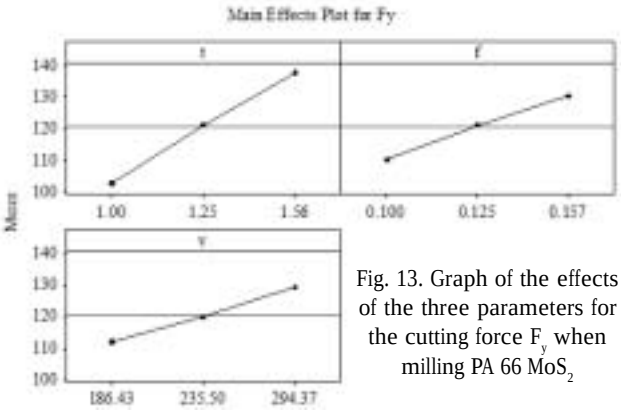

Fig. 13. Graph of the effects of the three parameters for the cutting force F_y when milling PA 66 MoS_2

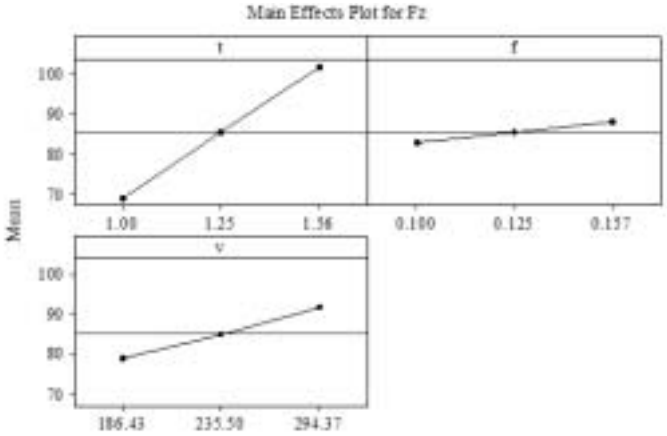

Fig. 14. Graph of the effects of the three parameters for the cutting force F_z when milling PA 66 MoS_2

Component Parameters	F_x P-value [%]	F_x Contribution [%]	F_y P-value [%]	F_y Contribution [%]	F_z P-value [%]	F_z Contribution [%]
t	0	72.92	0	58.02	0	74.19
f	0	20.17	0	19.68	6.3	1.86
v	0.1	4.62	0	14.38	0	11.26
t·f	52.2	0.37	0.1	4.59	0.8	6.99
t·v	15.3	0.97	1.3	2.17	44.4	0.97
f·v	93	0.09	30.7	0.49	8.4	2.86

Table 7
ANOVA ANALYSIS OF F_x, F_y,F_z FOR PA 66 MoS_2

The equations for the milling cutting force components are of the form:

$$F_x = -93.2326 + 66.9851 \cdot t + 186.996 \cdot f + 0.213197 \cdot v \ [N]. \quad (14)$$

For this model, the correlation coefficient R^2 is 97.28%. The Durbin-Watson statistic index is 2.28.

$$F_y = 67.215 - 22.9665 \cdot t + 84.6553 \cdot z - 0.148014 \cdot v + 208.565 \cdot t \cdot z + 0.241844 \cdot t \cdot v \ [N]. \quad (15)$$

For this model, the correlation coefficient R^2, used to establish the quality of the model, is 93.4%. The Durbin-Watson statistic index is 1.1.

$$F_z = 122.399 - 5.84398 \cdot t - 0.171758 \cdot v + 502.393 \cdot t \cdot z \ [N]. \quad (16)$$

For this model, the correlation coefficient R^2, used to establish the quality of the model, is 92.3%. The Durbin-Watson statistic index is 1.34.

In order to make a comparison between the size of the main component F_y and the other two components, F_x and F_z, mathematical calculations were made which resulted in the following relations:

$$F_x = (0.20 - 0.43) F_y \ [N]. \quad (17)$$

$$F_z = (0.59 - 0.89) F_y \ [N]. \quad (18)$$

To gain an insight into the differences between the size of the forces calculated experimentally and the ones obtained through modeling, the relative error was calculated using relation (8). In the case of PA 66 MoS_2, the maximal relative errors calculated were: 12.95% for F_x, 7.02% for F_y and 9.22% for F_z.

For the experimenting conditions established, regarding the material and the geommetry of the cutting plate, the material to process and the parameters of the cutting process, the size of the cutting force components, calculated using the relations 3,4,5,9,10,11,14,15,16, is summarized in table 8. For each material, the minimal, the mean, and the maximal values calculated were considered.

Figure 15 shows the eolution of the size of the main cutting force component, F_y, by number of experiment for the three materials analysed.

Material	PA66			PA66 GF 30			PA 66 MoS		
Force component	F_x	F_y	F_z	F_x	F_y	F_z	F_x	F_y	F_z
Minimal value	19.64	68.17	60.47	19.83	49.2	34.74	14.22	92.24	62.83
Maximal value	50.28	168.99	104.22	77.7	250	156.68	60.4	161.62	136.19
Mean value	28.53	118.97	83.64	44.47	139.45	76.65	38.77	120.55	85.86

Table 8
SIZE OF THE CUTTING FORCE COMPONENTS RESULTED FROM CALCULATIONS $-F_x,F_y,F_z$ [N]

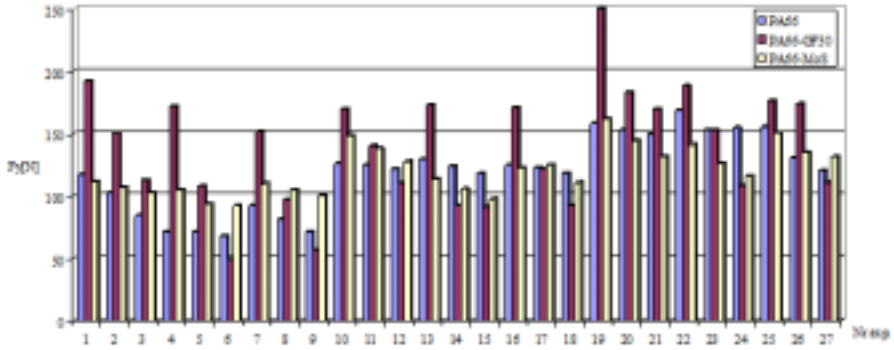

Fig. 15. Variation of the main cutting force component, F_y, by number of experiment and material

Validation of the cutting force model calculated experimentally for PA 66-GF 30

In order to validate the cutting force model of the plane milling of a PA 66-GF 30 part, the values of the working condition under which the specimen was processed were introduced in relation (10): t=1.4 m/min, f_{th}= 0.13 mm/th and v=200 m/min, resulting in

$$F_{ycalculated} = -409.391 + 134.118 \cdot t + 1130.08 \cdot f + + 1.690 \cdot v - 0.374 \cdot t \cdot v - 3.536 \cdot f \cdot v = 126.3 \text{ [N]} \quad (19)$$

The force measured was $F_{ymeasured} = 132.5[N]$.

To gain an insight into the differences between the size of the forces calculated experimentally and the ones obtained through modeling, the relative error was calculated using relation (8). In the case of PA 66-GF 30, the error calculated was: 4.68% for the parameters of the working condition presented above.

Conclusions

There have been conducted experimental research on the influence of the cutting condition on the size of the cutting milling force components. The work aimed to obtain the equations that define the variation of the cutting force components depending on the cutting condition parameters when processing specimens of polyamides PA66, PA66-PA66 GF30 and MoS_2.

Also, in order to make a comparison between the size of the main component, F_y and the other two components, F_x and F_z, mathematical calculations were made, resulting in dependence relations between them.

The experiments, which took into account the material and the geometry of the cutting plate, the material to process and the parameters of the cutting condition, allowed to establish the following conclusions:

- in terms of the size of the forces, it is observed that: the **F_x component** varies between 19.64 N and 50.28 N for the base material **PA 66**, between 19.83 N and 77.7 N for **PA 66-GF 30**, and between 14.22 N and 60.4 N for **PA 66 MoS_2**; the **F_y component** varies between 68.17 N and 168.99 N for the base material **PA 66**, between 49.2 N and 250 N for **PA 66-GF 30**, and between 92.24 N and 161.62 N for **PA 66 MoS_2**; the **F_z component** varies between 60.47 N and 104.22 N for the base material **PA 66**, between 34.74 N and 156, 68 N for **PA 66-GF 30**, and between 63.83 N and 136.19 N for **PA 66 MoS_2**. When processing each material, the parameters of the cutting condition were varied, namely the cutting speed, the feed and the cutting depth;

- the descending order of the size of the cutting forces was: **PA 66-GF 30**, **PA 66** and **PA 66 MoS_2**, as can be seen in figure 15. The smallest forces were recorded when processing polyamide PA66 MoS_2, due to the reinforcement element MoS_2, which provides good cutting properties to the material. When processing polyamide PA66-GF30, the existence of the glass-fiber results in an increase of the cutting force in comparison with the processing of polyamide PA66, by approximately 32.4%.

Research results are very useful for industrial scale processing, because they allow for the determination of the optimal parameters of the cutting condition with a view to obtaining a certain cutting force.

References

1. VASILE, Gh., FETECAU, C., SERBAN, A., Experimental Research On The Roughness Of Surfaces Processed Through Milling Polyamide Composites, Mat. Plast., **51**, no.2, 2014, p. 205

2. FETECAU, C., STAN, F., Study Of Cutting Force And Surface Roughness In Turning Of Polytetrafluoroethylene Composites With A Polycrystalline Diamond Tool, Measurement 45, Issue 6, July 2012, Elsevier, ISBN 0236-2241, 2012, p. 1367-1379.

3. VLAD, D., FETECAU, C., DOICIN, C., PALADE, I.L., Experimental Study On The Cutting Forces In Ptfe Orthogonal Cutting, Mat. Plast., **50**, no.4, 2013, p. 326.

4. PALADE, L., REIMANIS, E., GRAHAM, A., GOTTLIEB, M., Linear Viscoelastic Behaviour Of Highly Crosslinked Silica Reinforced Poly (Dimethyl-Siloxane) Rubbers, Mat. Plast., **50**, no.1, 2013, p. 1

5.STAN, F., Simulation Of Delamination Using Discontinuous Galerkin Finite Element Methods And Cohesive Models, Advances in Fracture and Damage Mechanics VIII Book Series: Key Engineering Materials Volume: 417-418, 2010, p. 501-504.

6.DAVIM, J.P., REIS, P., LAPA, V., ANTONIO, C. Machinability Study On Polyetheretherketone (Peek) Unreinforced And Reinforced (Gf30) For Applications In Structural Components. Compos Struct 62, 2003, p. 67–73

7.DAVIM, J.P, PEDRO, R.C., CONCEICAO, A., A Study On Milling Of Glass Fiber Reinforced Plastics Manufactured By Hand-Lay Up Using Statistical Analysis (Anova), Composite Structures 64, 2004, p. 493–500

8.DAVIM, J.P., MATA, F., New Machinability Study Of Glass Fiber Reinforced Plastics Using Polycrystalline Diamond And Cemented Carbide (K15) Tools, Materials & Design, Sciencedirect, London, 2007, p. 1050-1054

9.ZAMAN, M.T., SENTHIL, K.A., RAHMAN, M., SREERAM, S., A Three – Dimensional Analytical Cutting Force Model For Micro End Milling Operation. Int J. Machine Tools Manuf. vol 46, 2006, p. 353 – 66

10.STAN, F., Evaluation Of Dynamic Fracture Toughness And Weibull Master Curves Of Polymethyl Methacrylate, Mat. Plast., **54**, no. 1, 2008, p. 8

11.MATHUKRISHNAN, N., DAVIM, J.P., Optimization Of Machining Parameters Of Al/Sic-Mmc With Anova And Ann Analysis, Jmpt., 209, 2009, p.225-232.
12.QUADRINI, F., SQUEO, E. A., TAGLIAFERRI, V., Machining Of Glass Fiber Reinforced Polyamide, Express Polymer Letters Vol.1, nr.12, 2007, p. 810–816
13. XIAO, K.Q., XIAO, L.C., ZHANG, The Role Of Viscous Deformation In The Machining Of Polymers, International Journal of Mechanical Sciences, 44, 2002, p. 2317–2336
14.*** www.ceproinv.ro
15. JEYAKUMAR, S., MARIMUTHU, K., RAMACHANDRAN, T., Prediction of cutting force, tool wear and surface roughness of Al6061/SiC composite for end milling operations using RSM, Journal of Mechanical Science and Technology 27, nr.9, 2013, p. 2813-2822
16. KUMAR, S., MEENU, SATSANGI, P. S, Multiple-response optimization of turning machining by the Taguchi method and the utility concept using uni-directional glass fiber-reinforced plastic composite and carbide (k10) cutting tool, Journal of Mechanical Science and Technology 27, nr.9 ,2013, p. 2829- 2837
17. MIHAELA, E. ULMEANU, M., E., DOICIN, C., V., BAILA, D., I., ALLAN E.W., RENNIE, A., E., W., NEAGU., C., LAHA., S., Comparative Evaluation of Optimum Additive Manufacturing Technology to Fabricate Bespoke Medical Prototypes of Composite Materials, Mat. Plast., **52**, no.3, 2015, p. 416

Manuscript received: 4.12.2015